Adaptive LOS Path Following based on Trajectory Linearization Control for Unmanned Surface Vehicle with Multiple Disturbances and Input Saturation

Bingbing Qiu * Guofeng Wang * Yunsheng Fan * Dongdong Mu * Xiaojie Sun *

* *Marine Electrical Engineering College, Dalian Maritime University, Dalian CO 116026, China, (e-mail: bbqiu.dmu@gmail.com, gfwangsh@163.com, yunsheng@dlmu.edu.cn, ddmu.phd@gmail.com, xjsun.phd@gmail.com).*

Abstract: This paper develops an adaptive line-of-sight (LOS) path following control strategy for an unmanned surface vehicle (USV) subject to unknown multiple disturbances. An adaptive LOS guidance strategy is adopted to compensate for the sideslip angle induced by wind, waves and ocean currents. On the basis of considering the saturation of the actuator, a practical path following controller based on linear extended state observer (LESO) is presented by trajectory linearization control (TLC) technology and nonlinear tracking differentiator. The greatest advantage of this article is that the TLC technology is introduced into the field of USV motion control to design path following controller, which provides a new research field for the development of TLC. A feedback linearization control law is designed to enhance TLC technology in linear time-varying system, and a LESO is constructed to provide the estimates of the tracking errors and unknown disturbances. Meanwhile, to avoid signal hopping and reduce the consumption of control, the nonlinear tracking differentiator (NTD) is constructed to realize the derivative of virtual control command, which can also provide command filtering. In addition, auxiliary dynamic system is used to handle input saturation issue. Theoretical analysis illuminates that our scheme ensures the boundedness of all signals in the closed-loop systems. At last, the simulation results confirm the superior performance of the proposed strategy.

Keywords: USV, adaptive LOS, TLC technology, NTD, LESO, path following, feedback linearization.

1. INTRODUCTION

In recent years, USV has become gradually to be a hotspot of research. This is mainly due to its advantages of being fast, small volume, low cost, and the ability of autonomous navigation. USV has been successfully applied in many fields, such as ocean surveillance, search, rescue and military (Liu et al., (2018); Song et al., (2017)). However, it has a weak anti-interference ability due to its own attributes, particularly in the presence of unknown multiple disturbances during path following. Therefore, it is very important to design a path following controller with anti-interference capability.

For the development of USV, it is severely depended on these three kinds of technologies: setpoint control, trajectory tracking and path following. Setpoint control is driving the control objective from any initial point to a target point (Dong et al.,(2005); Do.(2010)). Trajectory tracking is defined as a control objective which is must required to follow a reference path with spatial and temporal constraint, namely, reference path with an associated time law (Zhu al.,(2018); Yang et al.,(2014); Guerrero al.,(2018); Suvire al.,(2017); Wang al.,(2017)). Path following is concerned with steering a control objective to follow a scheduled path by independently tracking a expected speed assignment and orientation control (Peymani et al., (2015); Hu et al.,(2016)). Compared with trajectory tracking, path following is easier to control and closer to practical applications. Therefore, the study of path following has practical value. Considerable researches have been conducted to investigate and address the path following control problems (Shin et al.,(2017); Zheng et al.,(2017)). Based on Serret-Frenet frame and backstepping technology, a state- and output-feedback controller is developed for path following of underactuated ships in (Do et al.(2004)) ,which is proved to be asymptotically stable at the origin. In addition, a popular method is to implement a line-of-sight (LOS) guidance algorithm, which is applied to obtain convergence to the desired path (Fossen et al.(2015)). Owing to the simplicity and effectiveness of the LOS guidance law, which has been successfully applied to the design of path following controller (Xiang et al.,(2012); Borhaug et al.,(2008); Lekkas et al.,(2014); Fossen et al.,(2017)). However, in practice, a nonzero sideslip angle is produced due to the influence of ocean currents, wind and waves, which reduces the performance of path following controller. Therefore, the influence of the sideslip angle should be considered in controller design.

To solve the above problem, many researchers have made a lot of efforts. First, the straightforward way is to measure sideslip angle. By measuring longitudinal and lateral accelerations, the sideslip angle is calculated in (Hac et al., (2000)). The drawback is that the noise and the measurement error are relatively large. In (Bevly et al., (2001)), the sideslip angle is calculated by a global navigation satellite system. However, the measuring equipment is expensive, and the measurement accuracy cannot be guaranteed. Then another way is indirect method to solve the sideslip problem. The integral LOS guidance is proposed in (Borhaug et al., (2008); Lekkas et al., (2014); Fossen et al., (2017); Fossen et al., (2015)), which alleviates the effect of sideslip angle by adding an integral term into the classical LOS guidance law. However, it may reduce the stability of the system due to the influence of an integral term (Han., (2009)). For the time-varying sideslip angle, a reduced-order LESO is used to estimate and compensate for sideslip angle in (Liu et al., (2017)). Similarly, a predictor is used to handle the time-varying sideslip angle in (Liu et al., (2016)), which not only preserves the simplicity, but also enables smooth and fast identification of the vehicle sideslip angle. The disadvantage is that they are difficult to apply in practice due to the low speed. Based on the above analysis, an adaptive LOS guidance law (Mu et al., (2017)) is adopted to estimate and compensate for the sideslip angle in this paper. Compared with (Liu et al., (2016)), the adaptive LOS can reduce the amount of calculation to some extent.

Focusing on ship motion control, many excellent control algorithms are developed for USV, such as the back-stepping technique (Do et al.(2004)), sliding mode control (Sun et al.(2017)) and adaptive nonlinear control (Zhu al.,(2018)). However, the above controllers not only have complex structure, but also have poor control performance with the increase of disturbance. With the development of nonlinear control methods, the trajectory linearization control (TLC) technology has been proven to be an effective technique to handle tracking and disturbance problems, which consists of nonlinear dynamic inversion and a linear time-varying (LTV) feedback stabilization, and it also has a strong anti-interference ability. Owing to its simplicity and robustness, TLC technology has been successfully applied to the controlling of missiles (Mickle et al., (2001)), vehicle flight (Zhu et al., (2006)), helicopter (Zhu et al., (2012)) and fixed-wing vehicle (Adami et al., (2011)). However, TLC technology can only make the closed-loop system obtain local exponential stability along the nominal trajectory (Liu et al., (2007)). In order to overcome this drawback, various modified TLC strategies have been explored in (Liu et al., (2006); Zhu et al., (2008); Xue et al., (2008); Jiang et al., (2008); Shao et al., (2015); Shao et al., (2014); Shao et al., (2014)). The first methodology for improving TLC is the use of the adaptive neural network in (Liu et al., (2006)). Subsequent extensions to the adaptive neural network are proposed in (Zhu et al., (2008); Xue et al., (2008)), respectively. By using T-S fuzzy system, a robust adaptive TLC algorithm is proposed in (Jiang et al., (2008)). In the context of aforementioned literature, the key is to take advantage of the adaptive neural network and fuzzy logic to estimate and compensate for the system uncertainties. However, too many design parameters not only increase the complexity of the design system but also may affect the control performance of the system. The second methodology is estimating and compensating the disturbances by using observers including reduced-order LESO (Shao et al., (2015);), sliding-mode disturbance observer (SMDO) (Shao et al., (2014)) and extended disturbance observer (EDO) (Shao et al., (2014)). In (Shao et al., (2015)), the system uncertainty is estimated and compensated by designed model-assisted reduced-order ESO. SMDO is constructed to estimate and counteract system uncertainties in (Shao et al., (2014)), but the drawback is that there exists a tremor phenomenon. For the uncertainties caused by using a new sliding surface, EDO is employed to eliminate the effect of uncertainties in (Shao et al., (2014)). In addition, in order to be closer to reality, input saturation (Zhu al.,(2018)) is considered in controller design, which is a common problem for the path following since the commanded control input calculated by the controller exceeds the physical limitations of the propulsion system. Many previous literatures did not consider input saturation, which would lead to decline or collapse of control system. Therefore, it is important to consider input saturation in practice.

In this paper, motivated by the existing results, a novel robust path following control scheme is performed according to adaptive LOS guidance strategy, TLC technology, LESO and auxiliary dynamic system. The following summarizes the main contributions of this paper:

(1) TLC technology is an effective control technique, which has strong anti-interference and robustness. Through the author's view, the TLC technology is a new control method in the design of path following controller for USV.

(2) To get closer to practical engineering, an adaptive LOS guidance strategy is employed to compensate for the sideslip angle. An auxiliary dynamic system is introduced to handle the problem of input saturation, and LESO is used to estimate the tracking errors and unknown disturbances. In addition, a NTD is adopted to avoid signal hopping in control input, which not only can reduce the consumption of control but also provide filter for input command.

(3) A feedback linearization (FL) control law instead of traditional TLC controller is used to stabilize a LTV system. As a result, only two parameters need to be tuned in our proposed scheme, which reduces the difficulty of adjusting the controller.

The rest of the paper is organized as follows. Section 2 proposes an adaptive LOS guidance law. In Section 3, a novel path following control strategy is developed for USV. Section 4 gives the stability of the system. Simulation results and comparisons are considered in Section 5. Section 6 concludes this paper and introduces future research.

2. ADAPTIVE LOS GUIDANCE ALGORITHMS

In this section, the adaptive LOS guidance scheme is designed to compensate for sideslip angle. If the sideslip angle produced by drift force is not properly compensated, the drift force significantly affects USV tracking performance and even deteriorates it.

2.1 Problem Formulation

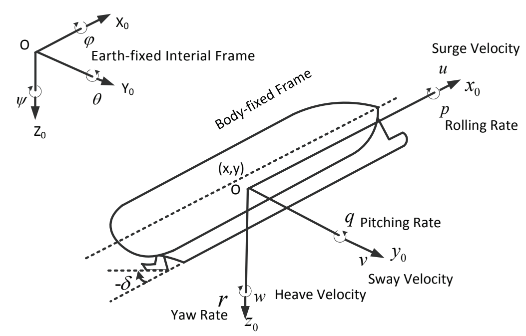

Fig. 1. The earth-fixed inertial and the body-fixed frame.

The horizontal plane motion of USV is described by the position and orientation, namely, neglecting rolling rate p, pitching angle q and heave velocity w. In Fig.1, $O - X_0Y_0Z_0$ is the earth-fixed inertial frame $\{i\}$ and $o - x_0y_0z_0$ is the body-fixed frame $\{b\}$. In addition, (x, y) denotes the position of USV in $\{b\}$; u, v and r represent the surge velocity, sway velocity and yaw rate, respectively. From (Jia et al., (1999)), the kinematics equation transformation between $\{i\}$ and $\{b\}$ can be written as

$$\dot{\eta}=J(\psi)\,v \tag{1}$$

where ψ is heading angle, $\eta = [x, y, \psi]^T$, $v = [u, v, r]^T$. $J(\psi) = \begin{bmatrix} \cos(\psi) & -\sin(\psi) & 0 \\ \sin(\psi) & \cos(\psi) & 0 \\ 0 & 0 & 1 \end{bmatrix}$ is transition matrix.

The USV kinematics equation can be rewritten as the following state-space equation

$$\begin{cases} \dot{x} = u\cos\psi - v\sin\psi \\ \dot{y} = u\sin\psi + v\cos\psi \\ \dot{\psi} = r \end{cases} \tag{2}$$

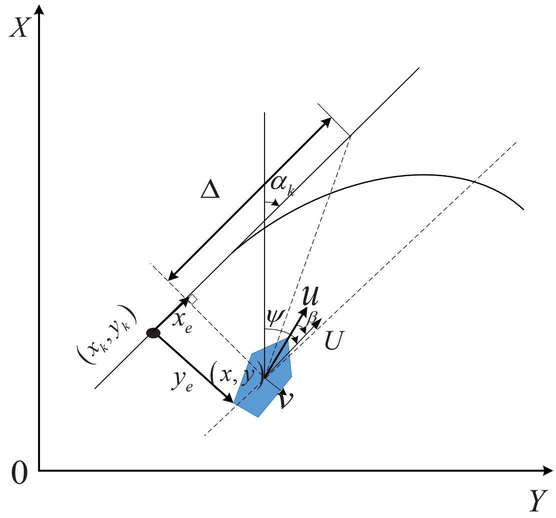

Fig. 2. Geometrical illustration of LOS guidance.

In Fig. 2, USV is located at (x, y). A geometric path $(x_k(\omega), y_k(\omega))$ is used as the reference path, in which ω denotes the path variable. In addition, the path-tangential angle $\alpha_k(\omega) = \mathrm{atan2}(y'_k(\omega), x'_k(\omega))$, where $x'_k(\omega) = \partial x_k/\partial\omega$, $y'_k(\omega) = \partial y_k/\partial\omega$.

Based on the above analysis, the along-track error x_e and the cross-track error y_e in XOY can be expressed as

$$\begin{bmatrix} x_e \\ y_e \end{bmatrix} = \begin{bmatrix} \cos\alpha_k & -\sin\alpha_k \\ \sin\alpha_k & \cos\alpha_k \end{bmatrix}^T \begin{bmatrix} x - x_k(\omega) \\ y - y_k(\omega) \end{bmatrix} \tag{3}$$

Taking the time derivative of x_e yields

$$\begin{aligned} \dot{x}_e &= \dot{x}\cos\alpha_k + \dot{y}\sin\alpha_k \\ &\quad - \dot{x}_k(\omega)\cos\alpha_k - \dot{y}_k(\omega)\sin\alpha_k \\ &\quad + \dot{\alpha}_k \underbrace{\left[-(x - x_k(\omega))\sin\alpha_k + (y - y_k(\omega))\cos\alpha_k\right]}_{y_e} \end{aligned} \tag{4}$$

In the light of (2), (4) can be expressed as

$$\begin{aligned} \dot{x}_e &= u\cos(\psi - \alpha_k) - v\sin(\psi - \alpha_k) + \dot{\alpha}_k y_e \\ &\quad - \dot{\omega}\sqrt{{x'_k}^2(\omega) + {y'_k}^2(\omega)}\cos(\alpha_k + \phi) \\ &= U\cos(\psi - \alpha_k + \beta) + \dot{\alpha}_k y_e - u_p \end{aligned} \tag{5}$$

where $\phi = \mathrm{atan2}(-y'_k(\omega), x'_k(\omega)) = -\alpha_k$, $U = \sqrt{u^2 + v^2} > 0$ is the speed of USV, and $\beta = \mathrm{atan2}(v, u)$ denotes the sideslip angle. In addition, u_p is the virtual reference speed to stabilize x_e, which is defined as

$$u_p = \dot{\omega}\sqrt{{x'_k}^2(\omega) + {y'_k}^2(\omega)} \tag{6}$$

Similarly, differentiating y_e along (3) gives

$$\begin{aligned} \dot{y}_e &= -\dot{x}\sin\alpha_k + \dot{y}\cos\alpha_k \\ &\quad + \dot{x}_k(\omega)\sin\alpha_k - \dot{y}_k(\omega)\cos\alpha_k \\ &\quad - \dot{\alpha}_k \underbrace{\left[-(x - x_k(\omega))\cos\alpha_k + (y - y_k(\omega))\sin\alpha_k\right]}_{x_e} \end{aligned} \tag{7}$$

Substituting (2) into (7) yields

$$\dot{y}_e = U\sin(\psi - \alpha_k + \beta) - \dot{\alpha}_k x_e \tag{8}$$

Note that the sideslip angle β is quite small (Fossen et al.(2015)) and slowly time-varying, and this means that $\sin(\beta) = \beta$, $\cos(\beta) = 1, \dot{\beta} \approx 0$.

Therefore, we have

$$\begin{cases} \dot{x}_e = U\cos(\psi - \alpha_k) - U\sin(\psi - \alpha_k)\beta + \dot{\alpha}_k y_e - u_p \\ \dot{y}_e = U\sin(\psi - \alpha_k) + U\cos(\psi - \alpha_k)\beta - \dot{\alpha}_k x_e \end{cases} \tag{9}$$

The design objective is to propose an adaptive LOS guidance law which the USV with the kinematics (2) to follow a reference path $(x_k(\omega), y_k(\omega))$ such that the unknown sideslip can be compensated with the guaranteed performance. Specifically, the design objective is to achieve $x_e \to 0$ and $y_e \to 0$ as $t \to 0$.

2.2 Guidance Law Design

Assumption 1. The heading controller can follow the desired heading angle perfectly such that ψ=ψ_d.

Therefore, the adaptive LOS guidance law is proposed as

$$\psi_d = \alpha_k(\omega) + \arctan\left(-\frac{y_e}{\Delta} - \hat{\beta}\right) \tag{10}$$

$$\dot{\hat{\beta}} = \sigma\frac{U\Delta y_e}{\sqrt{\Delta^2 + \left(y_e + \Delta\hat{\beta}\right)^2}} \tag{11}$$

where σ is a positive design parameter, $\hat{\beta}$ is the estimate of β.

To stabilize x_e, u_p is selected as

$$u_p = U\frac{\left(y_e + \Delta\hat{\beta}\right)\beta + \Delta}{\sqrt{\Delta^2 + \left(y_e + \Delta\hat{\beta}\right)^2}} + \lambda_0 x_e \tag{12}$$

where λ_0 is a constant parameter.

From (6), $\dot{\omega}$ is expressed as

$$\dot{\omega} = \frac{u_p}{\sqrt{{x'_k}^2(\omega) + {y'_k}^2(\omega)}} \tag{13}$$

where $0 < \Delta_{\min} < \Delta < \Delta_{\max}$ is specified lookahead distance. Applied to (9) with $0 < U_{\min} \le U \le U_{\max}$ renders the origin $\left(x_e, y_e, \tilde{\beta}\right) = (0, 0, 0)$ uniformly globally asymptotically stable (UGAS), and $\tilde{\beta} = \beta - \hat{\beta}$ represents estimation error.

Noting

$$\sin\left(\arctan\left(-\frac{y_e+\Delta\hat{\beta}}{\Delta}\right)\right) = -\frac{y_e+\Delta\hat{\beta}}{\sqrt{\Delta^2+\left(y_e+\Delta\hat{\beta}\right)^2}} \tag{14}$$

$$\cos\left(\arctan\left(-\frac{y_e+\Delta\hat{\beta}}{\Delta}\right)\right) = \frac{\Delta}{\sqrt{\Delta^2+\left(y_e+\Delta\hat{\beta}\right)^2}} \tag{15}$$

From the above analysis, $\dot{x}_e$ and $\dot{y}_e$ can be expressed as

$$\begin{cases} \dot{x}_e = U\frac{(y_e+\Delta\hat{\beta})\beta+\Delta}{\sqrt{\Delta^2+(y_e+\Delta\hat{\beta})^2}} - u_p + \dot{\alpha}_k y_e \\ \dot{y}_e = -U\frac{y_e-\Delta\tilde{\beta}}{\sqrt{\Delta^2+(y_e+\Delta\hat{\beta})^2}} - \dot{\alpha}_k x_e \end{cases} \tag{16}$$

Consider the Lyapunov function

$$V_1 = \frac{1}{2}x_e^2 + \frac{1}{2}y_e^2 + \frac{1}{2\sigma}\tilde{\beta}^2 \tag{17}$$

The derivative of V_1 with respect to (16) satisfies

$$\begin{aligned} \dot{V}_1 &= x_e\dot{x}_e + y_e\dot{y}_e + \frac{1}{\sigma}\tilde{\beta}\dot{\tilde{\beta}} \\ &= -\lambda_0 x_e^2 - \frac{U y_e^2}{\sqrt{\Delta^2+\left(y_e+\Delta\hat{\beta}\right)^2}} \\ &\quad + \tilde{\beta}\left(\frac{U\Delta y_e}{\sqrt{\Delta^2+\left(y_e+\Delta\hat{\beta}\right)^2}} + \frac{1}{\sigma}\dot{\tilde{\beta}}\right) \end{aligned} \tag{18}$$

Since $\dot{\tilde{\beta}} = -\dot{\hat{\beta}}$, then substituting (11) into (18) yields

$$\dot{V}_1 < -\lambda_0 x_e^2 - \frac{U y_e^2}{\sqrt{\Delta^2+\left(y_e+\Delta\hat{\beta}\right)^2}} < 0 \tag{19}$$

The speed of USV is selected as

$$U = \zeta\sqrt{\Delta^2+\left(y_e+\Delta\hat{\beta}\right)^2} \tag{20}$$

where $\zeta > 0$, one can get that

$$\dot{V}_1 \le -\lambda_0 x_e^2 - \zeta y_e^2 < 0 \tag{21}$$

Theorem 1. Suppose ω, ψ_d and U can satisfy (13), (10) and (20), respectively, so the origin $\left(x_e, y_e, \tilde{\beta}\right) = (0,0,0)$ is uniformly globally exponentially stable (UGES).

Proof. By the stability theory of Lyapunov, let V_1 be positive define and radially unbounded. In the case of (13), (10) and (20), the derivative of V_1 is quadratically negative definite. Hence, $\left(x_e, y_e, \tilde{\beta}\right) = (0,0,0)$ is UGES. However, this is an ideal conclusion, and it is hard to realize in practice.

3. CONTROL DESIGN

Considering the actual navigation of USV, the following Norrbin nonlinear model (Li, (2008)) describing the USV dynamic characteristics is expressed as

$$\begin{cases} \dot{\psi} = r \\ \dot{r} = -\frac{1}{T}r - \frac{\alpha}{T}r^3 + \frac{K}{T}\delta + \Delta d \end{cases} \tag{22}$$

where α is the Norrbin coefficient, T and K are the maneuverability index of USV; Δd represents unknown multiple disturbances and δ is the rudder angle. In practice, considering the saturation characteristics of the USV rudder, the limitation of δ can be described as

$$\delta = \begin{cases} \delta_{\max}, & if\ \delta_0 > \delta_{\max} \\ \delta_0, & if\ \delta_{\min} < \delta_0 < \delta_{\max} \\ \delta_{\min}, & if\ \delta_0 < \delta_{\min} \end{cases} \tag{23}$$

where $\delta_{\max}$ and $\delta_{\min}$ are the maximum and minimum output, δ_0 is the control command calculated by enhanced TLC control law.

In this subsection, our main purpose is to design a novel control input δ in the presence of unknown multiple disturbances and input saturation, so that the actual heading angle ψ tracks the heading angle ψ_d produced by the adaptive LOS guidance algorithm.

Assumption 2. The desired heading ψ_d is bounded, and its first, second order derivative are available.

Assumption 3. The multiple disturbances Δd are bounded, $|\Delta d| \leqslant \Delta d_{\max}$ with $\Delta d_{\max}$ is unknown positive constant.

3.1 TLC Technology

Define $X = [X_1, X_2]^T = [\psi, r]^T$, $F_1(X) = \left[X_2, -\frac{1}{T}X_2 - \frac{\alpha}{T}X_2^3\right]^T$, $G_1 = \left[0, \frac{K}{T}\right]^T$, $G_2 = [0,1]^T$, $Y = h(X) = X_1$, and the system (22) can be rewritten as a single input single output (SISO) nonlinear system

$$\begin{cases} \dot{X} = F_1(X) + G_1\delta + G_2\Delta d \\ Y = h(X) \end{cases} \tag{24}$$

In addition, there exists a G_0, which satisfies

$$G_1 G_0 = G_2 \tag{25}$$

Without consideration of multiple disturbances, we define X^*, Y^*, $\bar{\delta}$ as the nominal state, nominal output and nominal input, respectively. Then the nominal trajectory can be expressed as

$$\begin{cases} \dot{X}^* = F_1(X^*) + G_1\bar{\delta} \\ Y^* = h(X^*) \end{cases} \tag{26}$$

According to the design principle of TLC, the control law of TLC can be written as

$$\delta_0 = \bar{\delta} + \tilde{\delta} \tag{27}$$

where $\tilde{\delta}$ is an LTV control law.

The structure of TLC technology is described in Fig. 3, and it mainly consists of two parts: (1) A dynamic inverse controller is adopted to calculate $\bar{\delta}$; (2) The LTV feedback regulator $\tilde{\delta}$ keeps the system stable and has a certain response characteristics.

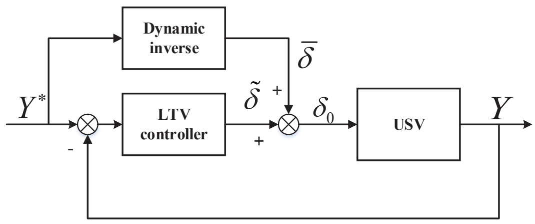

Fig. 3. TLC scheme diagram.

Define the tracking error $E = \left[X_1 - X_1^*, X_2 - X_2^*\right]^T$, the time derivative of E is

$$\begin{aligned}\dot{E} &= F_1\left(X^* + E\right) + G_1\left(\bar{\delta} + \tilde{\delta}\right) \\ &\quad - F_1\left(X^*\right) - G_1\bar{\delta} \\ &= F\left(X^*, \bar{\delta}, E, \tilde{\delta}\right)\end{aligned} \tag{28}$$

From the TLC control theory (Khalil, (1996)), X^* and $\bar{\delta}$ in (28) can be considered as two time-varying parameters, and we have

$$\begin{aligned}\dot{E} &= F\left(X^*, \bar{\delta}, E, \tilde{\delta}\right) \\ &= F\left(t, E\right)\end{aligned} \tag{29}$$

Linearizing (29) along the nominal trajectory $\left(X^*, \bar{\delta}\right)$ yields the tracking error

$$\dot{E} = A_1 E + B_1 \tilde{\delta} \tag{30}$$

where $A_1 = \left(\frac{\partial F_1}{\partial X} + \frac{\partial G_1}{\partial X}\delta\right)|_{X^*,\bar{\delta}}$, $B_1 = G_1|_{X^*,\bar{\delta}}$.

Remark 1. From (Shao et al., (2014); Khalil, (1996)), we can know that the system (29) is continuous differential and bounded, and A_1, B_1 are completely controllable.

In order to stabilize tracking error, by using differential algebraic spectrum theory (Mickle et al., (1997); Zhu, (1997)), the LTV feedback control law can be designed as

$$\tilde{\delta} = K_\delta E \tag{31}$$

where K_δ represents feedback gain matrix.

Then the closed loop tracking error can be written as

$$\dot{E} = A_c E \tag{32}$$

where $A_c = \begin{bmatrix} 0 & 1 \\ -\tau_{j1} & -\tau_{j2} \end{bmatrix}$, in which $\tau_{j1} > 0, \tau_{j2} > 0\,(j = 1)$ can be gained from the second-order LTV differential equation (Adami et al., (2011)). If the PD-eigenvalues satisfy $\rho_1 = -\left(\varsigma_j \pm \sqrt{1 - \varsigma_j^2}\right) w_{nj}$, we have

$$\begin{aligned}\tau_{j1} &= w_{nj}^2 \\ \tau_{j2} &= 2\varsigma_j w_{nj} - \frac{\dot{w}_{nj}}{w_{nj}}\end{aligned} \tag{33}$$

where ς_j is the constant damping, w_{nj} is the constant damping.

Therefore, the traditional TLC control law can be rewritten as

$$\delta_0 = \bar{\delta} + K_\delta E \tag{34}$$

3.2 Structure of the Proposed Control Scheme

Fig. 4 demonstrates the structure of the proposed novel path following control scheme for USV with unknown multiple disturbances. It mainly consists of two parts: the first part is that the LOS guidance strategy compensates for the sideslip angle, and it can also provide a desired path; The second part is the enhance TLC controller which consists of pseudo-dynamic inverse controller (open-loop control) and a FL controller (close-loop control). Meanwhile, NTD is used to overcome the shortcomings of SOLD, which not only realizes the derivatives of the nominal states wherever it is needed, but also provides command filtering. In addition, the input saturation is solved using an auxiliary design system. In order to improve control performance of the system, LESO is employed to estimate external disturbance to achieve real-time compensation.

3.3 TLC Controller Design

In this section, a nonlinear open-loop controller is designed according to the structure of TLC, which can be obtained (without uncertainties) by inverting (26) as

$$\bar{\delta} = G_1{}^{\dagger}\left(\dot{X}^* - F\left(X^*\right)\right) \tag{35}$$

where X^* is obtained by the second-order linear differentiator (SOLD), † denotes the pseudo inverse operator defined as $P^\dagger = P^T\left(P^T P\right)^{-1}$, and $\bar{\delta}$ is nominal control rudder angle.

In the traditional TLC design, SOLD is used to produce X^* and $\dot{X}^*$ by the nominal input X^{ref}, which has been used in many literatures (Liu et al., (2006); Zhu et al., (2008); Xue et al., (2008); Jiang et al., (2008)), and SOLD can be expressed as

$$\begin{cases} \dot{z}_1 = z_2 \\ T_m \dot{z}_2 = -\left(z_1 - X^{ref}\right) - 2T_m z_2 \\ y = z_2 \end{cases} \tag{36}$$

where T_m is the time constant.

It is obvious that $\lim\limits_{T_m \to 0} z_1 = X^{ref} = X^*$, $\lim\limits_{T_m \to 0} z_2 = \dot{X}^{ref} = \dot{X}^*$. When the initial conditions of $z_1(0)$ and $X^{ref}(0)$ have large errors, due to the high gain influence of the differentiator, the derivative of $X^{ref}(0)$ will produce a peak phenomenon during transient phase. Similarly, the nominal differential signal $\dot{X}^*$ and input $\bar{\delta}$ also have signal hopping, which will cause large control input instantaneously. Therefore, to deal with the above problems, a nonlinear tracking differentiator (Han, (2009); Gao, (2004)) is used to replace SOLD in this paper. The specific form of TD is expressed as

$$\begin{cases} fh = fhan\left(X^*(k) - X^{ref}(k), \dot{X}^*(k), r_1, h_0\right) \\ X^*(k+1) = X^*(k) + h_1 \cdot \dot{X}^*(k) \\ \dot{X}^*(k+1) = \dot{X}^*(k) + h_1 \cdot fh \end{cases} \tag{37}$$

where h_0 is a control parameter, h_1, r_1 denote the sampling period and acceleration factor, respectively. The peak of the differential signal is regulated by acceleration factor r_1 in NTD. Therefore, it can avoid the peak phenomenon in linear differentiator.

Then, a FL based controller is developed to stabilize LTV system. In the presence of unknown multiple disturbances, the differential of tracking errors can be represented as

$$\dot{E} = A_1 E + B_1 \tilde{\delta} + G_2 \Delta d \tag{38}$$

For (38), if the system uncertainties are known, the controller can be designed by a FL method as

$$\begin{aligned}\tilde{\delta} &= B_1{}^{\dagger}\left(-A_1\right)E - \vartheta - K_1 E) \\ K_1 &= diag\left(K_{11}, K_{12}\right)\end{aligned} \tag{39}$$

where $\vartheta = G_2 \Delta d$, and $K_{11} > 0$, $K_{12} > 0$ are the design parameters.

To eliminate the effect of the system uncertainties, a LESO is constructed to estimate ϑ. In the framework of LESO, we define X_3 as an extended state vector of ϑ, and (38) becomes

$$\begin{aligned}\dot{E} &= A_1 E + B_1 \tilde{\delta} + X_3 \\ \dot{\vartheta} &= G(t)\end{aligned} \tag{40}$$

where $G(t)$ is the derivative of ϑ. Then a particular LESO of (40) is given as

$$\begin{aligned}\tilde{E} &= E - \hat{E} \\ \dot{\hat{E}} &= \hat{\vartheta} + l_1 \tilde{E} + \left(A_1 E + B_1 \tilde{\delta}\right) \\ \dot{\hat{\vartheta}} &= l_2 \tilde{E}\end{aligned} \tag{41}$$

where $\hat{\vartheta}$ represents the estimate of ϑ, its estimation error is $\tilde{\vartheta} = \vartheta - \hat{\vartheta}$. $\tilde{E}$ and $\hat{E}$ represent the estimation error and the

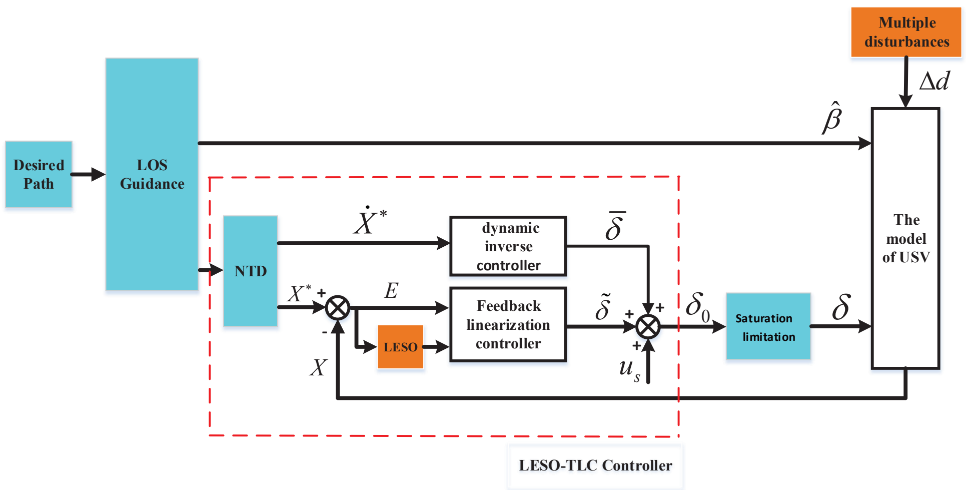

Fig. 4. The structure of the proposed path following control scheme for USV.

estimate value of E, respectively. In addition, $l_1^{2\times 2}$ and $l_2^{2\times 2}$ are the tuning matrices, which satisfy (Zheng et al., (2012))

$$\lambda_{01}(s) = \prod_{i=1}^{2}\left(s^2 + l_{1i}s + l_{2i}\right) = \prod_{i=1}^{2}(s+\omega_{1i})^2 \tag{42}$$
$$l_j = diag\left(l_{j1}, l_{j2}\right)(j=1,2), \omega_1 = diag(\omega_{11}, \omega_{12})$$

where ω_{1i} is the bandwidth of LESO. From (40) and (41), the differential of the estimation errors can be expressed as

$$\begin{aligned}\dot{\tilde{E}} &= \tilde{\vartheta} - l_1\tilde{E}\\ \dot{\tilde{\vartheta}} &= G(t) - l_2\tilde{E}\end{aligned} \tag{43}$$

Then (43) can be written as a form of state space

$$\dot{E}_\Omega = A_{01}E_\Omega + B_{01}G(t) \tag{44}$$

where $E_\Omega = \left[\tilde{E}, \tilde{\vartheta}\right]^T = \left[E-\hat{E}, \vartheta-\hat{\vartheta}\right]^T$, $A_{01}=\begin{bmatrix}-l_1I_2 & I_2\\ -l_2I_2 & 0_2\end{bmatrix}$, $B_{01} = \begin{bmatrix}0\\ I_2\end{bmatrix}$, in which I_2 is identity matrix. In addition, A_{01} is Hurwitz.

Theorem 2. Suppose that $G(t)$ is bounded, there exists a constant C_1 such that $\|G(t)\| \le C_1$. Then $\|E_\Omega\|$ of (44) is bounded, which satisfies $\|E_\Omega\| \le C_2$ as $t \to \infty$, where $C_2 > 0$.

Proof. For A_{01} of (44), if there exist four different negative real eigenvalues such that $-\tau_1 < ... < -\tau_4 < 0, \tau_i > 0\,(i = 1...4)$, so there exists nonsingular matrix Γ, which satisfies

$$A_{01} = \Gamma diag\{-\tau_1, -\tau_2, -\tau_3, -\tau_4\}\Gamma^{-1} \tag{45}$$

Note that

$$\begin{aligned}\exp(A_{01}t) = \Gamma diag\{&-\exp(\tau_1 t), -\exp(\tau_2 t),\\ &-\exp(\tau_3 t), -\exp(\tau_4 t)\}\Gamma^{-1}\end{aligned} \tag{46}$$

First, m_∞ norm is selected for the matrix norm ($t > 0$). Obviously, $\left\|\exp(A_{01}t)\right\|_{m_\infty} \le \kappa\exp(-\tau_1 t)\,(\kappa > 0)$. So (44) can be written as

$$\begin{aligned}E_\Omega(t) &= \exp(A_{01}t)E_\Omega(0)\\ &+ \int_0^t \exp(A_{01}(t-\lambda))B_{01}G(t)\,d\lambda, t > 0\end{aligned} \tag{47}$$

Therefore, one can get that

$$\begin{aligned}\|E_\Omega(t)\| \le\ & \left\|\exp(A_{01}t)E_\Omega(0)\right\|\\ &+ \left\|\int_0^t \exp(A_{01}(t-\lambda))B_{01}G(t)\,d\lambda\right\|\\ &\le \left\|\exp(A_{01}t)\right\|_{m_\infty}\|E_\Omega(0)\|\\ &+ \int_0^t \left\|\exp(A_{01}(t-\lambda))\right\|_{m_\infty}\|B_{01}\|\,\|G(t)\|\,d\lambda\\ &\le \kappa\|E_\Omega(0)\|\exp(-\tau_1 t)\\ &+ \frac{C_1\kappa}{\tau_1}(1-\exp(-\tau_1 t))\\ &\le \frac{C_1\kappa}{\tau_1} = C_2\end{aligned} \tag{48}$$

Remark 2. Theorem 2 proves that the proposed LESO has good observational performance, and the estimation errors will become small enough by adjustment the design parameters of LESO. Moreover, under the controller (39), the system performance has a strong robustness even with a large disturbance.

Through the estimated value $\hat{\vartheta}$, the FL controller can be expressed as

$$\begin{aligned}\tilde{\delta} &= B_1{}^{\dagger}\left(-A_1E - \hat{\vartheta} - K_1E\right)\\ K_1 &= diag(K_{11}, K_{12})\end{aligned} \tag{49}$$

Remark 3. K_{11} and K_{12} are chosen by time-varying parallel differential (PD) spectral theory in (Qiu et al., (2018); Qiu et al., (2019)), and tuning parameters are a complex process. To simplify this process, an enhance TLC technology is developed in this paper, in which a novel FL control law replaces traditional LTV control law to stabilize a LTV system. The pole assignment technique is used to regulate the closed-loop error dynamics, which makes the desired characteristic polynomial satisfy $s^2 + K_{11}s + K_{12}=(s+\omega_c)^2$. Note that the enhance TLC technology just needs a tuning parameter, which is more convenient for engineering implementation. In addition, in the absence of the integral action, the novel FL controller can also eliminate the tracking errors.

To solve input saturation problem, an auxiliary design system is constructed in the paper, which can be rewritten as

$$\dot{\Theta} = \begin{cases} -K_\Theta\Theta - \frac{|E\cdot o\delta|+0.5o\delta^2}{\|\Theta^2\|}\cdot\Theta + o\delta, & \|\Theta\| > \chi_1\\ 0, & \|\Theta\| < \chi_1\end{cases} \tag{50}$$

where K_Θ is a design parameter, Θ is an auxiliary variable, $o\delta = \delta - \delta_0$, and $\chi_1 > 0$ is a small parameter.

The control law δ_0 can be expressed as

$$\delta_0 = \bar{\delta} + \tilde{\delta} + u_s \tag{51}$$

where $u_s = k_s\Theta$, k_s is a positive design parameter.

4. STABILITY ANALYSIS

Theorem 3. For the tracking error E of the closed-loop system, under the control law (51), which can converge to a residual set of the origin, that is, tracking error E is uniformly ultimately bounded (UUB).

Proof. The Lyapunov function is constructed as following

$$V_2 = \frac{1}{2}E^T E + \frac{1}{2}\Theta^2 \tag{52}$$

Differentiating (52) and substituting (38) into (52) yields

$$\begin{aligned}\dot{V}_2 &= E^T\dot{E} + \Theta\dot{\Theta} \\ &= E^T\left(A_1E + B_1\tilde{\delta} + G_2\Delta d\right) + \Theta\dot{\Theta}\end{aligned} \tag{53}$$

Substituting (49) into (53), one can get that

$$\begin{aligned}\dot{V}_2 &= E^T\left(\vartheta - \hat{\vartheta} - K_1E\right) + \Theta\dot{\Theta} \\ &= E^T\left(\tilde{\vartheta} - K_1E\right) + \Theta\dot{\Theta} \\ &= -E^TK_1E + E^T\tilde{\vartheta} + \Theta\dot{\Theta}\end{aligned} \tag{54}$$

It is clear that

$$\Theta\dot{\Theta} = -K_\Theta\Theta^2 - \frac{|E\cdot o\delta| + 0.5o\delta^2}{\left\|\Theta^2\right\|}\cdot\Theta^2 + o\delta\cdot\Theta \tag{55}$$

$$o\delta\cdot\Theta \le \frac{1}{2}o\delta^2 + \frac{1}{2}\Theta^2 \tag{56}$$

Then

$$\dot{V}_2 \le -E^TK_1E + E^T\tilde{\vartheta} - |E\cdot o\delta| - \left(K_\Theta - \frac{1}{2}\right)\Theta^2 \tag{57}$$

From Young's inequality, we have

$$\begin{aligned}\dot{V}_2 &\leqslant -E^TK_1E + E^T\tilde{\vartheta} - |E\cdot o\delta| - \left(K_\Theta - \frac{1}{2}\right)\Theta^2 \\ &\leqslant -\lambda_{\min}(K_1)\|E\|^2 + \frac{1}{2}\left\|E^T\right\|^2 + \frac{1}{2}\left\|\tilde{\vartheta}\right\|^2 \\ &+ \frac{1}{2}\|E\|^2 + \frac{1}{2}|o\delta|^2 - \left(K_\Theta - \frac{1}{2}\right)\Theta^2 \\ &\leqslant -(\lambda_{\min}(K_1) - 1)\|E\|^2 - \left(K_\Theta - \frac{1}{2}\right)\Theta^2 \\ &+ \frac{1}{2}\left\|\tilde{\vartheta}\right\|^2 + \frac{1}{2}|o\delta|^2\end{aligned} \tag{58}$$

Set $\gamma_1 = \lambda_{\min}(K_1) - 1 > 0$, $\gamma_2 = K_\Theta - \frac{1}{2} > 0$, $\nabla = \frac{1}{2}\left\|\tilde{\vartheta}\right\|^2 + \frac{1}{2}|o\delta|^2$, (58) becomes

$$\dot{V}_2 \leqslant -\gamma_1\|E\|^2 - \gamma_2\Theta^2 + \nabla \tag{59}$$

Define $\gamma = \min\{\gamma_1, \gamma_2\}$, we have

$$\dot{V}_2 \leqslant -2\gamma V_2 + \nabla \tag{60}$$

Solving inequality (60) gives

Table 1. Initial Conditions and Controller Parameters.

	Parameter Value
The initial conditions of USV	$[x(0), y(0), \psi(0)] = [0m, 100m, 0rad]$, $[u(0), v(0), r(0)] = [6m/s, 0m/s, 0m/s]$, $\delta_{\max} = 35$ degree, $\delta_{\min} = -35$ degree.
the proposed scheme	$K_\Theta = 0.8$, $\chi_1 = 0.95$, $\Delta = 30$, $\lambda_0 = 30$, $\sigma = 0.001$, $\omega_c = 2$, $\omega_1 = 5I$, $K_{11} = \omega_c^2$, $K_{12} = 2\omega_c$, $l_1 = 2\omega_1$, $l_2 = \omega_1^2$, $k_s = 1$.
NTD	$h_0 = 0.2$, $h_1 = 0.02s$, $r_1 = 0.06rads^{-2}$.
traditional TLC technology	$\omega_{diff} = 4$, $T_{diff} = 1$, $w_{n1} = 2$, $\varsigma_1 = 0.7$.
ADRC method	$h_0 = 0.04$, $r_0 = 0.08$, $K_d = 8$, $K_p = 10$, $l_1 = 10$, $l_2 = 80$, $l_3 = 2$, $\alpha_1 = 0.72$, $\alpha_2 = 1.2$, $\varepsilon = 0.25$.

$$\begin{aligned}\dot{V}_2 &\leqslant \left(V_2(0) - \frac{\nabla}{2\gamma}\right)e^{-2\gamma t} + \frac{\nabla}{2\gamma} \\ &\leqslant V_2(0)e^{-2\gamma t} + \frac{\nabla}{2\gamma}\end{aligned} \tag{61}$$

Based on the above analysis, it is obviously seen that $V_2(t)$ is eventually bounded by $\frac{\nabla}{2\gamma}$, thus E is UUB.

Theorem 4. For a closed-loop system composed of (2), (22), (10), (11), (51), there exist appropriate design parameters σ, λ_0, K_{11}, K_{12}, ω_c, l_1, l_2, k_s, so all error values are UUB.

Proof. The Lyapunov function candidate be given by

$$V = V_1 + V_2 \tag{62}$$

From (21) and (59), one can get that

$$\dot{V} \leqslant -\lambda_0 x_e^2 - \xi y_e^2 - \gamma_1\|E\|^2 - \gamma_2\Theta^2 + \nabla \tag{63}$$

Therefore, $\dot{V}$ is a negative definite bounded, and all error values in the path following system are UUB.

5. SIMULATION RESULTS AND COMPARISON

To evaluate the effectiveness of the proposed control strategy, the "Lanxin" USV of Dalian Maritime University is selected as the research object, and the detailed parameters are obtained through model identification in (Mu et al., (2018)). For comparison, two controllers are given as follows: traditional TLC (Adami et al., (2011)) and active disturbance rejection control (ADRC) (Huang al., (2017)). Meanwhile, the control parameters and initial conditions are illustrated in Table 1. In order to better show the application of theory, Fig. 5 proposes a simulation validation diagram, and the specific steps are:

1) First, an adaptive LOS guidance law $\dot{\hat{\beta}}$ and the desired heading angle ψ_d are provided through the LOS guidance algorithm.

2) Based on heading angle ψ_d, three controllers are developed according to the enhanced TLC, the traditional TLC and ADRC methods, respectively.

3) Finally, the straight-line and curve simulations are carried out using MATLAB software platform.

Remark 4. On the basis of traditional TLC, an enhance TLC technology is developed in this paper. In addition, the ADRC

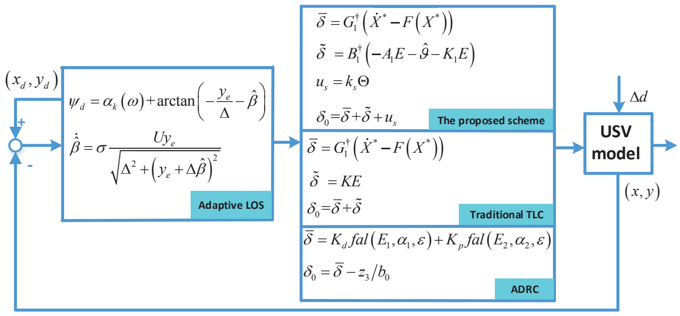

Fig. 5. Simulation validation diagram.

method is one of the most classical algorithms in path following control of USV, which consists of TD, conventional ESO and nonlinear state error feedback (NLSEF). Therefore, they are very persuasive to compare the proposed scheme.

5.1 Straight-Line Path Following

First, the straight-line path following simulation is carried out, and the desired path is a straight-line expressed as $[x_d, y_d] = [\omega, \omega]$. In addition, the multiple disturbances (Panet al., (2013)) are selected as

$$\Delta d = 0.1{+}0.1\sin(0.1t) + 0.2\cos(0.2t) \tag{64}$$

The straight-line path simulation results are demonstrated in Fig. 6 - Fig. 11.

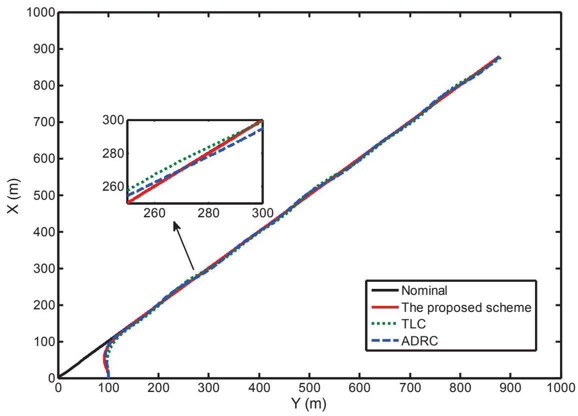

Fig. 6. Results of the straight-line path following.

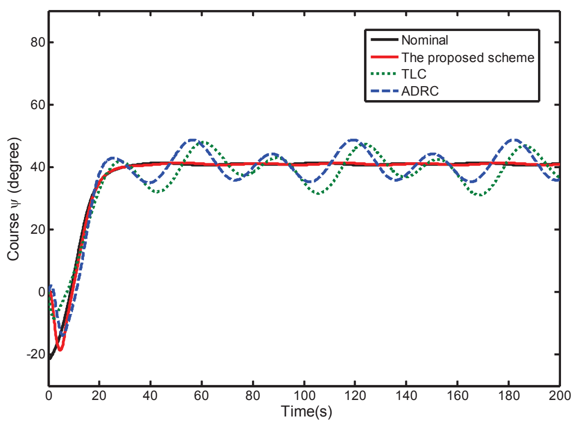

Fig. 7. Heading results of the straight-line path following.

In Fig. 6 - Fig. 11, the black the dash line represents the given straight-line path, and the red lines, the green dots, the dash

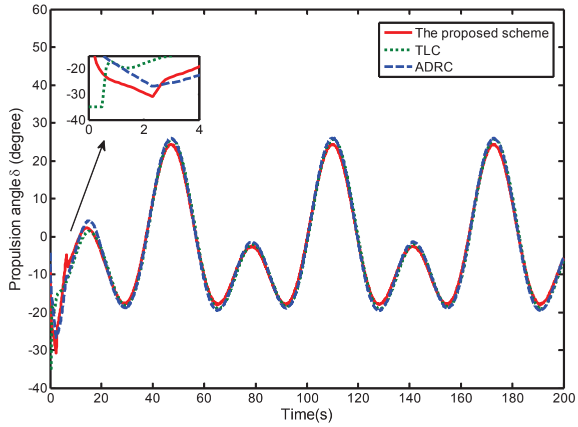

Fig. 8. Rudder angle results of the straight-line path following.

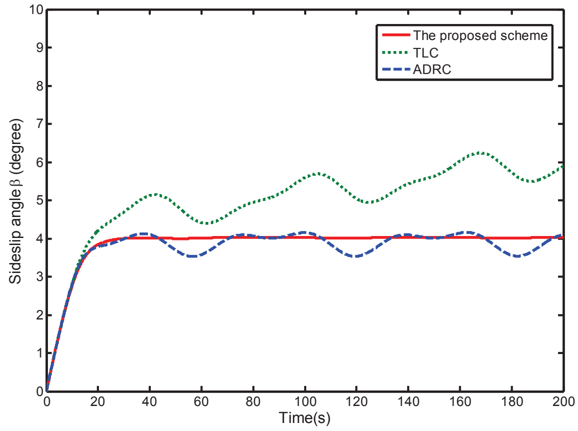

Fig. 9. Sideslip angle results of the straight-line path following.

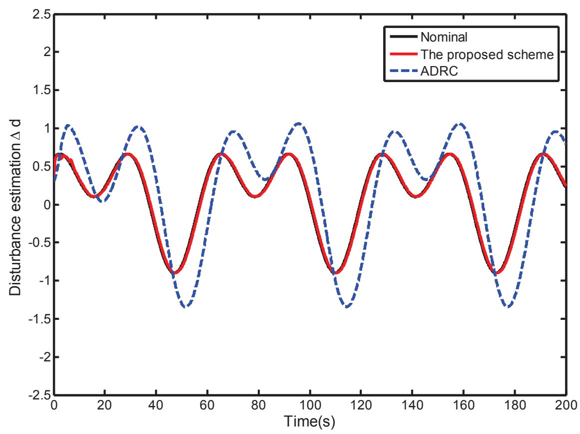

Fig. 10. Disturbance estimation results of the straight-line path following.

lines represent the proposed scheme , the TLC and the ADRC results, respectively. From Figs. 6 and 7, it can be clearly observed that the proposed scheme has better performance in control quality, especially in the tracking precision and robustness. Fig. 8 shows the comparisons between control inputs δ. It is obviously observed that the dramatic peak phenomenon (input saturation) is observed from the response of the rudder angle in TLC method, which is caused by the derivative of virtual control command. Because NTD and the auxiliary design system is used in the proposed scheme and ADRC method, input saturation phenomenon is directly avoided, and much smaller

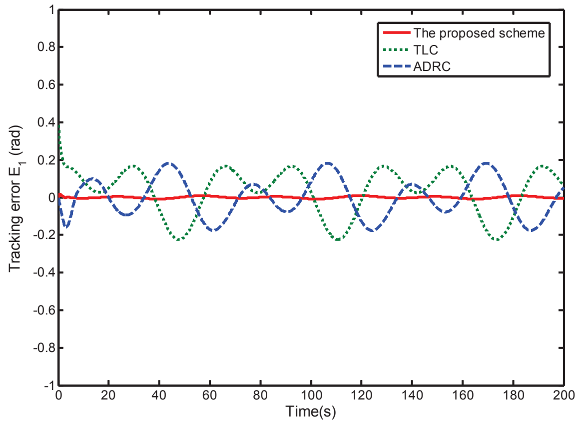

Fig. 11. Tracking error results of the straight-line path following.

deflection angles are generated. Fig. 9 clearly demonstrates that the sideslip angle of the proposed scheme eventually converges to a fixed value, and it keeps steady in the vicinity of 4 degree. However, the sideslip angle of TLC and ADRC methods have large fluctuation. From Fig. 10, we can see that the the proposed scheme can accurately estimate the disturbance. In addition, Fig. 11 demonstrates that tracking error of the proposed scheme converges to zero quickly and eventually maintains stable near zero. But tracking errors of TLC and ADRC methods are still fluctuating. Therefore, based on the presented and analyzed results, we can conclude that the proposed scheme has a strong tracking performance and robustness.

5.2 *Curve Path Following*

Then the curve path following simulation is carried out. Meanwhile, all parameters and conditions remain the same, and the desired curve path is $[x_d, y_d] = [200\sin(\omega/100), \omega]$. The curve path simulation results are shown in Fig. 12 - Fig. 17.

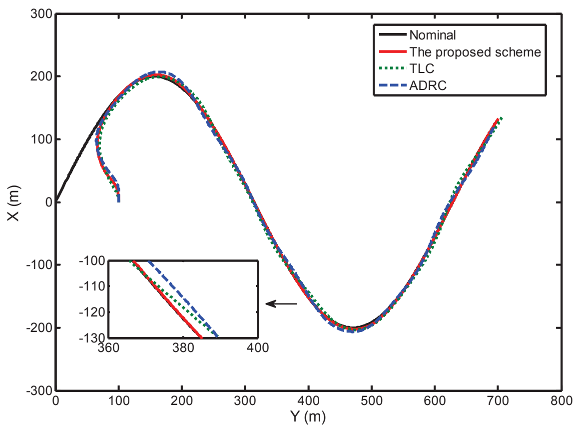

Fig. 12. Results of the curve path following.

Fig. 12 and Fig. 13 demonstrate that the USV still tracks the given curve path and heading accurately under multiple disturbances, which illustrate that the control performance of the proposed scheme is the best in the comparison. From Fig. 14, it can also observe that the input saturation immediately appears at the beginning. The main reason is that the derivative of control command produce a peak phenomenon. The input saturation is delayed or directly avoided in the proposed scheme and ADRC methods due to the use of NTD and the auxiliary

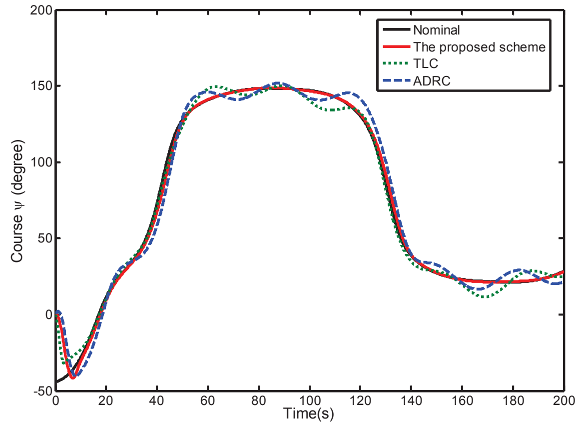

Fig. 13. Heading results of the curve path following.

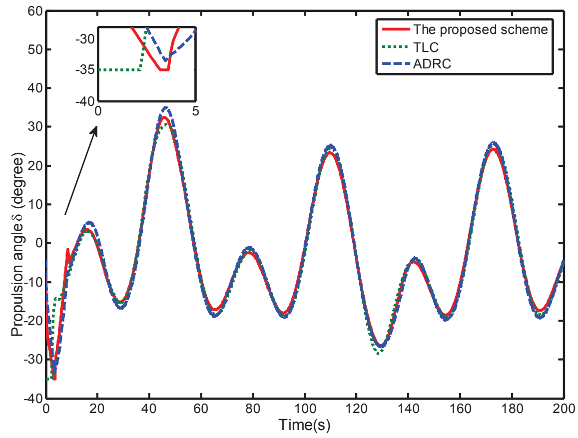

Fig. 14. Rudder angle results of the curve path following.

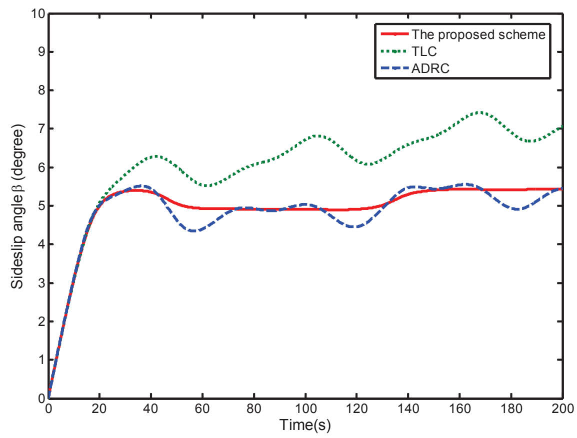

Fig. 15. Sideslip angle results of the curve path following.

design system, and fewer control consumption is achieved. Therefore, the problem of the input saturation needs to be considered. Similarly, Fig. 15 shows that the estimated values of sideslip angle eventually converge to 5 degree under the proposed scheme. Fig. 16 demonstrates that the proposed scheme has a good performance of the disturbance estimation. Fig. 17 shows the comparisons between tracking errors, which clearly demonstrate that the proposed scheme has better tracking performance. Therefore, based on the presented and analyzed results, we can conclude that when considering the performance of the controllers in all aspects of a control system such as

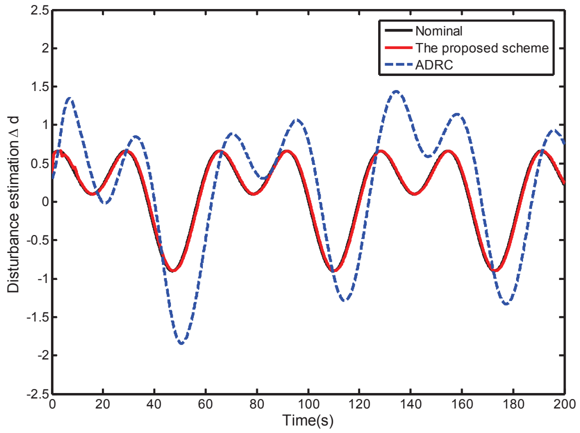

Fig. 16. Disturbance estimation results of the curve path following.

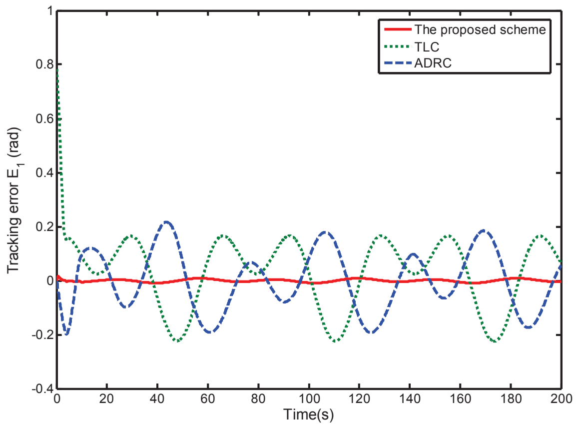

Fig. 17. Tracking error results of the curve path following.

tracking error, control efforts and estimation performance, the proposed scheme is the best among compared controllers.

6. CONCLUSION

This paper has presented an adaptive LOS path following control strategy for USV with unknown multiple disturbances. Through the author's view, the major advantage is that the TLC technology is used as a new control method in USV control field. The path following controller is proposed by combing an adaptive LOS guidance strategy, TLC technology and LESO. Meanwhile, with NTD applied in the proposed method to substitute for SOLD, which makes the control saturation delay or avoid. In addition, the input saturation problem is considered by using an auxiliary design system. Finally, compared with TLC and ADRC methods, the simulation results validate the efficacy and performance of the proposed scheme for USV.

However, we still need to consider more many practical problems. For example, the sideslip angle may be time-varying, and the linearization errors are neglected. In addition, TLC technology can also be applied to more fields (Martin al.,(2009); Haidegger al.,(2012); Caramihai al.,(2017); Vrkalovic al.,(2018)). These problems will be solved in the following works.

ACKNOWLEDGEMENTS

This work was supported by "the Nature Science Foundation of China" (grand number 51609033), "the Nature Science Foundation of Liaoning Province of China" (grand number 20180520005), and "the Fundamental Research Funds for the Central Universities" (grand numbers 3132018306, 3132019005).

ABBREVIATIONS

The following abbreviations are used in this manuscript:

ADRC	active disturbance rejection control
ESO	extended state observer
EDO	extended disturbance observer
FL	feedback linearization
LOS	line-of-sight
LTV	linear time-varying
LESO	linear extended state observer
NTD	nonlinear tracking differentiator
NLSEF	nonlinear state error feedback
PD	parallel differential
SMDO	sliding-mode disturbance observer
SOLD	second-order linear differentiator
SISO	single input single output
TLC	trajectory linearization control
USV	unmanned surface vehicle
UGES	uniformly globally exponentially stable
UUB	uniformly ultimately bounded

REFERENCES

Adami, T., and Zhu, J. (2011). 6DOF flight control of fixed-wing aircraft by Trajectory Linearization. *American Control Conference. IEEE*, 1610–1617.

Borhaug, E., Pavlov, A., and Pettersen, K.Y. (2008). Integral LOS control for path following of underactuated marine surface vessels in the presence of constant ocean currents. *Proceedings of the IEEE Conference on Decision and Control*, 30(2), 4984–4991.

Bevly, D., Sheridan, R., and Gerdes, J. (2001). Integrating INS sensors with GPS velocity measurements for continuous estimation of vehicle sideslip and tire cornering stiffness. *American Control Conference*, 1(4), 25–30.

Caramihai, S., Dumitrache, I., Stanescu, A., and Culita, J. (2017). A cooperative enterprise agent based control architecture. *CoRR abs/1704.02935*.

Dong, W., and Guo, Y. (2005). Global time-varying stabilization of underactuated surface vessel. *IEEE Transactions on Automatic Control*, 50(6), 859–864.

Do, K. (2010). Practical control of underactuated ships. *Ocean Engineering*, 37(13), 1111–1119.

Do, K., and Pan, J. (2004). State- and output-feedback robust path-following controllers for underactuated ships using Serret-Frenet frame. *Ocean Engineering*, 31(5), 587–613.

Fossen, T.I, Pettersen, K.Y, and Galeazzi, R. (2015). Line-of-Sight Path Following for Dubins Paths With Adaptive Sideslip Compensation of Drift Forces. *IEEE Transactions on Control Systems Technology*, 23(2), 820–827.

Fossen, T., and Lekkas, M. (2017). Direct and indirect adaptive integral line-of-sight path-following controllers for marine craft exposed to ocean currents. *International Journal of Adaptive Control & Signal Processing*, 31(4), 445–463.

Guerrero, J., Torres, J., Antonio, E., and Campos, E. (2018). Autonomous Underwater Vehicle Robust Path Tracking: Generalized Super-Twisting Algorithm and Block Backstepping Controllers. *Control Engineering and Applied Informatics*, 20(2), 51–63.

Gao, Z. Q (2004). On discrete time optimal control: A closed-form solution. *Proceedings of the 2004 American Control Conference*, 1, 52–58.

Hu, C., Wang, R., Yan, F., and Chen, N. (2016). Robust Composite Nonlinear Feedback Path-Following Control for Underactuated Surface Vessels with Desired-Heading Amendment. *IEEE Transactions on Industrial Electronics*, 67, 44–52.

Hac, A., and Simpson, M. (2000). Estimation of vehicle side slip angle and yaw rate. *SAE Trans*, 109, 1032–1038.

Han, J. (2009). From PID to Active Disturbance Rejection Control. *IEEE Transactions on Industrial Electronics*, 56(3), 900–906.

Huang, H., and Fan, Y. (2017). Path Following for Unmanned Surface Vessels Based on Adaptive LOS Guidance and ADRC. *International Conference on Neural Information Processing*, 192–200.

Haidegger, T., Kovaacs, L., Precup, R., Benyo, B., Benyo, Z., and Preitl, S. (2012). Simulation and control for telerobots in space medicine. *Acta Astronautica*, 81(1), 390–402.

Jiang, C.S, Zhang, C., and Zhu, L. (2008). Research of robust adaptive trajectory linearization control based on T-S fuzzy system. *Journal of Systems Engineering and Electronics*, 19(3), 537–545.

Jia, X., Yang, Y. (1999). Mathematical model of ship motion. *In Dalian Maritime University press; Dalian, China*.

Khalil, H. (1996). Nonlinear Systems. *In Prentice Hall; New York, America*.

Liu, Y., and Bucknall. R. (2018). Efficient multi-task allocation and path planning for unmanned surface vehicle in support of ocean operations. *Neurocomputing*, 275, 1550-1566.

Lekkas, M., and Fossen, T. (2014). Integral LOS Path Following for Curved Paths Based on a Monotone Cubic Hermite Spline Parametrization. *IEEE Transactions on Control Systems Technology*, 22(6), 2287–2301.

Liu, L., Wang, D., and Peng, Z. (2017). ESO-Based Line-of-Sight Guidance Law for Path Following of Underactuated Marine Surface Vehicles With Exact Sideslip Compensation. *IEEE Journal of Oceanic Engineering*, 42(2), 477–487.

Liu, L., Wang, D., Peng, Z., and Wang, H. (2016). Predictor-based LOS guidance law for path following of underactuated marine surface vehicles with sideslip compensation. *Ocean Engineering*, 124, 340–348.

Liu, Y., and Zhu, J. (2007). Regular Perturbation Analysis for Trajectory Linearization Control. *Proceedings of the American Control Conference*, 3047–3052.

Liu, Y., Huang, R., and Zhu, J. (2006). Adaptive Neural Network Control Based on Trajectory Linearization Control. *Proceedings of the World Congress on Intelligent Control and Automation*, 1, 417–421.

Li, D. (2008). Ship motion and modeling. *In National Defense Industry Press, Beijing, China*, 326–374.

Mu, D., Wang, G., Fan. Y., Sun, X., and Qiu, B. (2017). Adaptive LOS Path Following for a Podded Propulsion Unmanned Surface Vehicle with Uncertainty of Model and Actuator Saturation. *Applied Sciences*, 7(12), 1232.

Mu, D., Wang, G., Fan. Y., Sun, X., and Qiu, B. (2018). Modeling and identification for vector propulsion of an unmanned surface vehicle: Three degrees of freedom model and response model. *Sensors*, 18(6).

Mickle, M., and Zhu, J. (2001). Skid to turn control of the APKWS missile using trajectory linearization technique. *American Control Conference*, 5, 3346–3351.

Mickle, M., and Zhu, J. (1997). Nonlinear missile planar autopilot design based on PD-spectrum assignment. *IEEE Conference on Decision and Control*, 4, 3914–3919.

Martin, D., Del Toro, R., Haber, R., and Dorronsoro, J. (2009). Optimal tuning of a networked linear controller using a multi-objective genetic algorithm and its application to one complex electromechanical process. *International Journal of Innovative Computing, Information and Control*, 5(10), 3405–3414.

Peymani, E., and Fossen, T. (2015). Path following of underwater robots using Lagrange multipliers. *Robotics and Autonomous Systems*, 67, 44–52.

Pan, C., Lai, X., Yang, S.,and Wu, M. (2013). An efficient neural network approach to tracking control of an autonomous surface vehicle with unknown dynamics. *Expert Systems with Applications*, 40, 1629–1635.

Qiu, B.B, Wang, G.F, Fan. Y.S, Mu, D.D, and Sun, X.J (2018). Path following controller design for unmanned surface vehicle based on trajectory linearization control. *International Journal of Innovative Computing, Information and Control*, 14(6), 2273–2290.

Qiu, B.B, Wang, G.F, Fan. Y.S, Mu, D.D, and Sun, X.J (2019). Robust Adaptive Trajectory Linearization Control for Tracking Control of Surface Vessels with Modeling Uncertainties under Input Saturation. *IEEE Access*, 7, 5057–5070.

Song, R., Liu, Y., and Bucknall. R. (2017). A multi-layered fast marching method for unmanned surface vehicle path planning in a time-variant maritime environment. *Ocean Engineering*, 129, 301-317.

Shin, J., Kwak, D., and Lee, Y. (2017). Adaptive path-following control for an unmanned surface vessel using an identified dynamic model. *IEEE/ASME Transactions on Mechatronics*, 22(3), 1143–1153.

Shao, X., and Wang,H. (2015). Back-stepping active disturbance rejection control design for integrated missile guidance and control system via reduced-order ESO. *Isa Transactions*, 57(4), 10–22.

Shao, X., and Wang,H. (2014). Attitude control of hypersonic vehicle based on SMDO-TLC. *Journal of Beijing University of Aeronautics and Astronautics*, 40(11), 1568-1575.

Shao, X., and Wang,H. (2014). Sliding mode based trajectory linearization control for hypersonic reentry vehicle via extended disturbance observer. *Isa Transactions*, 53(6), 1771–1786.

Shao, X., and Wang,H. (2014). A Novel Method of Robust Trajectory Linearization Control Based on Disturbance Rejection. *Mathematical Problems in Engineering*, 2014(6), 1–10.

Sun, Z.J., Zhang, G.Q., Yi,B.W, and Zhang,W.D. (2017). Practical proportional integral sliding mode control for underactuated surface ships in the fields of marine practice. *Ocean Engineering*, 142, 217–223.

Suvire, R., Serrano, M., Vega, J., Ortiz, O., and Scaglia, G. (2017). Nonlinear Controller for Trajectory Tracking of a Continuous Stirred Tank Reactor. *Control Engineering and Applied Informatics*, 19(4), 112–121.

Vrkalovic, S., Lunca, E.C., and Borlea, L.D. (2018). Model-Free Sliding Mode and Fuzzy Controllers for Reverse Osmosis Desalination Plants. *International Journal of Artificial Intelligence*, 16(2), 208–222.

Wang, H.P., Tian, Y., and Vasseur, C. (2017). State Feedback Trajectory Tracking Control of Nonlinear Affine in Control System with Unknown Internal Dynamics and Disturbances. *Control Engineering and Applied Informatics*, 19(3), 22–30.

Xiang, X., Liu, C., Lapierre, L., and Jouvencel, B. (2012). Synchronized path following control of multiple homogenous underactuated AUVs. *Journal of Systems Science & Complexity*, 25(1), 71–89.

Xue, Y., and Jiang, C. (2008). Trajectory linearization control of an aerospace vehicle based on RBF neural network. *Journal of Systems Engineering and Electronics*, 19(4), 799–805.

Yang, Y., Du, J., Liu, H., Guo, C., and Abraham, A. (2014). A trajectory tracking robust controller of surface vessels with disturbance uncertainties *IEEE Transactions on Control Systems Technology*, 22(4), 1511–1518.

Zhu, G.B., and Du, J.L. (2018). Global Robust Adaptive Trajectory Tracking Control for Surface Ships Under Input Saturation. *IEEE Jouranl of Oceanic Engineering*.

Zheng, Z., and Feroskhan, M. (2017). Path following of a surface vessel with prescribed performance in the presence of input saturation and external disturbances. *IEEE/ASME Transactions on Mechatronics*, 22(6), 2564–2575.

Zhu, J., Banker, B., and Hall, C. (2006). X-33 ascent flight control design by trajectory linearization - A singular perturbation approach. *Proceedings of the AIAA Guidance, Navigation, and Control Conference*.

Zhu, B., and Huo, W (2012). Adaptive Trajectory Linearization Control for a model-scaled helicopter with uncertain inertial parameters. *Control Conference. IEEE*, 4389–4395.

Zhu, L., Jiang, C., and Xue, Y. (2008). Robust Adaptive Trajectory Linearization Control for Aerospace Vehicle Using Single Hidden Layer Neural Networks. *Acta Armamentarii*, 29(1), 52–56.

Zhu, J. (1997). PD-spectral theory for multivariable linear time-varying systems. *IEEE Conference on Decision and Control*, 4, 3908–3913.

Zheng, Q., Gao, L., and Gao, Z. (2012). On Validation of Extended State Observer Through Analysis and Experimentation. *Journal of Dynamic Systems Measurement & Control*, 134(2), 1–6.